Supporting Information

Cancer Cell-Selective Promoter Recognition Accompanies Antitumor Effect by Glucocorticoid Receptor-Targeted Gold Nanoparticle

Samaresh Sau, Pritha Agarwalla†, Sudip Mukherjee†, Indira Bag, Bojja Shreedhar, Manika Pal-Bhadra, Chitta Ranjan Patra*, Rajkumar Banerjee*

Saturation curve and percent attachment of Dex and MDA:

To determine the amount of Dex and MDA to saturate GNP, we measured UV-Vis absorbance by adding Dex, from 0 to 100µg/ml concentration range in 600 ml of GNP, which contains 15 mg of gold. It has been observed that upto 50µg/ml of Dex addition; the absorbance of GNP increased sharply after that it slowly falls. So from this data we understand that GNP can be saturated by 50µg/ml of Dex. Similarly we have seen 100µg/ml is the saturation concentration of MDA with GNP. In GNP-formulations as used in the present manuscript, 50 percent saturation concentration of Dex (25ug/ml) and 25 percent saturation concentration of MDA (25µg/ml) have been used.

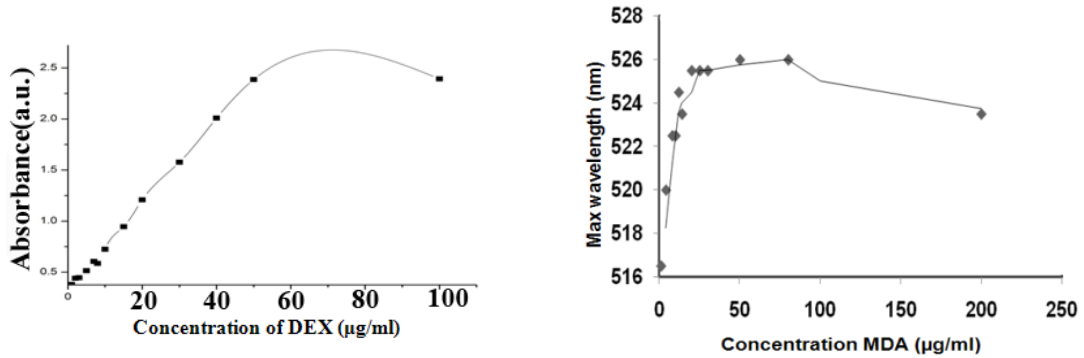

Figure S1: Saturation curve of Dex(**a**) and MDA(**b**) on GNP.

Change of UV-Vis absorbance of Dex in different conditions:

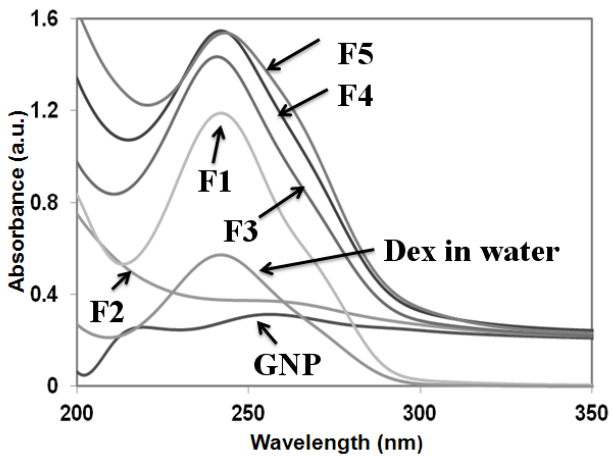

Figure S2. Absorbance (a.u.) of MDA in GNP (F2), Dex in water and in GNP-formulations (F3, F4, F5) or Dex and MDA in water (F1). The data indicates that there is a small red shift(2-3nm) of Dex λmax in case of F4-F5in comparison to than in F1 and the absorbance values of F4-F5 have increased by more than 2 folds in comparison to Dex in water and 1.3-1.4 times more than Dex and MDA combination (F1) .

Fourier Transformed infrared spectra (FTIR):

In order to understand the binding of MDA and Dex on GNP-surface, we did FTIR-spectroscopy of naked MDA and Dex as well as F2-F5. For this experiment we did centrifugation (Sorvall™ WX Floor Ultracentrifuges, USA) of all GNP-formulations (F2-F5), with 18000 rpm at 100c temperature. Then separated unattached MDA/Dex, and dried it. After that we made KBr pallets using this MDA/Dex containing GNP-conjugates and analysed in FTIR spectrophotometer (PerkinElmer, MA, USA). In Figure S2, figure (a) indicating FTIR of Dex and figure (b)indicating FTIR of F5, (c) indicating FTIR of F2, (d) indicating FTIR of MDA, (e) indicating FTIR of F3, (f) indicating FTIR of F4. The major stretching frequency of Dex is observed at 3471, 2939, 1703, 1662, 1618,1604 and 1453cm-1,where asF3, F4, and F5 showed in range of 3354-3364, 2920-2927, 2353-2366, 1648-1664, and 1559-1560cm-1. Here the major stretching frequency (υ)= 3471cm-1 of spectrum (a) is due to O-H stretching mode, which is significantly shifted downward at of 3354-3364 cm-1in spectrum (b e, f)as broadened peak, indicating the role of Dex 'O-H' in binding with GNP surface. Again sharp stretching frequency (υ) =1703, 1662cm-1 of spectrum (a) is due to carbonyls (C=O) functionality of Dex, which appears as weak peak at a range of 1648-1664cm-1 and 1559-1560cm-1is possibly due to interaction of dex carbonyl group with GNP surface. To understand attachment of MDA on GNP surface, it's found S-H stretching frequency at (2550-2600 cm-1) disappeared among all MDA-attached GNP; say F2, F4, F5 as marked by red arrow. Furthermore, please note that MDA binding (S-GNP chemisorptions) has an influence on asymmetric and symmetric stretching frequency of the –CH2 groups, as result stretching frequency of MDA at 1701cm-1is reduced to 1652-1664 cm-1 with narrowing of band. So these evidences indicate the bonding of MDA to GNP through S-H end.[1-4]

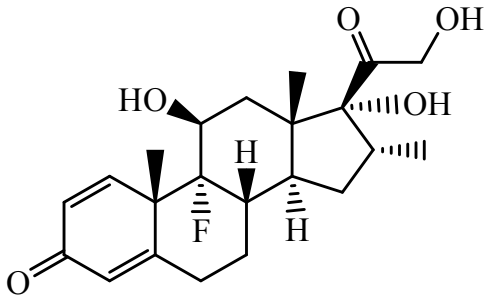

Dexamethasone (Dex)

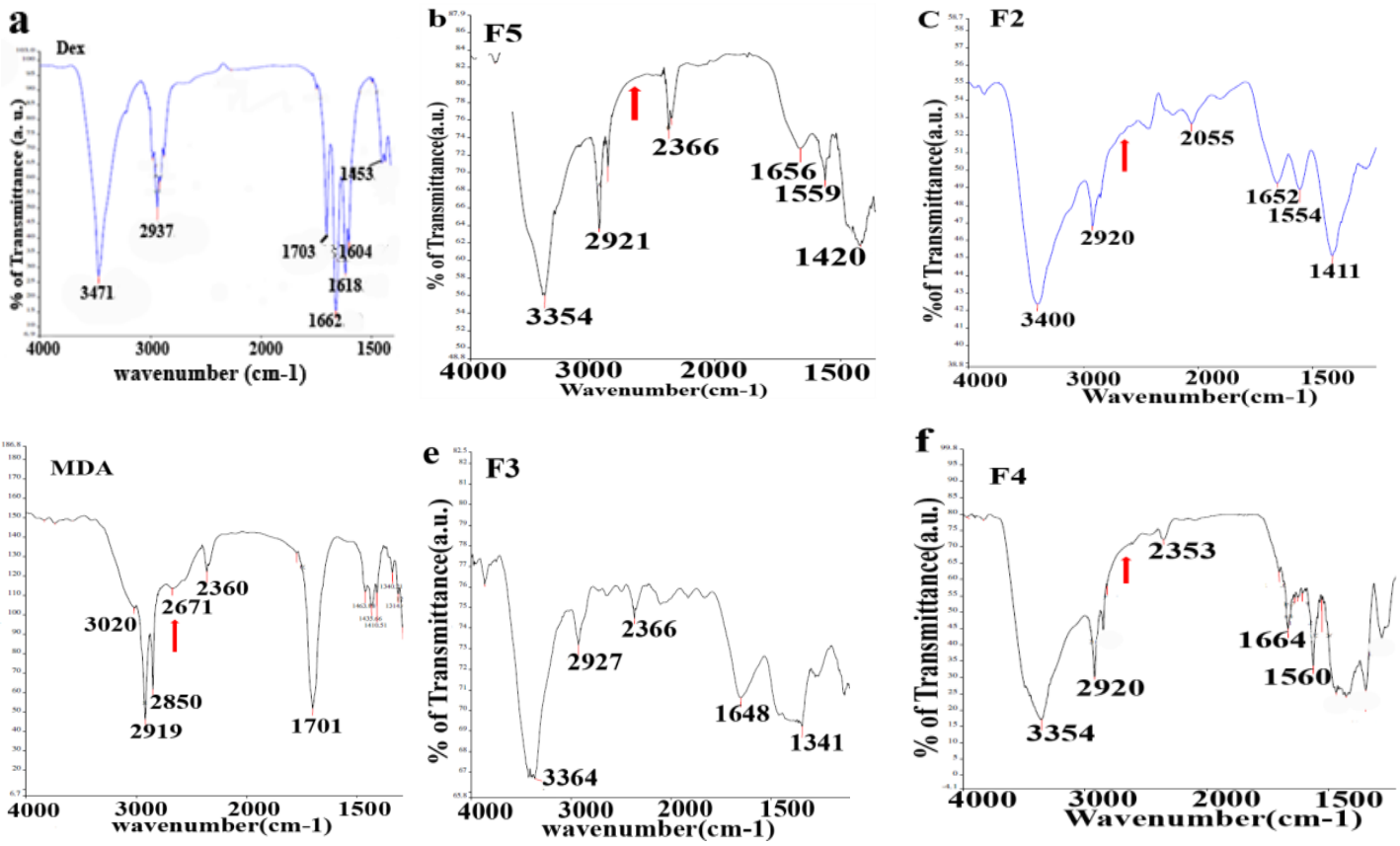

Figure S3: Fourier Transformed infrared spectra (FTIR) of Dex (a), F5 (b), F2(c), MDA (d), F3 (e), F4 (f).

X-ray diffraction (XRD) analysis: For X-ray diffraction (XRD) analysis, we made a F5-coated glass slide and dried it, then used for analysis.

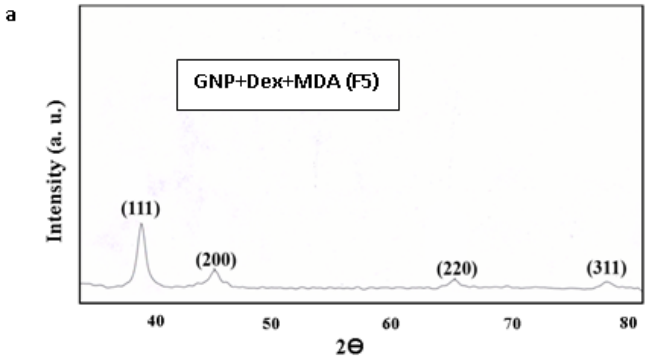

Figure S4: X-ray diffraction (XRD) pattern suggesting the crystal structure of F5- formulation is Face-centered cubic (FCC) phase of GNP. Hence crystal structure GNP is maintained after adsorption of Dex and MDA in F5-formulation (GNP+ Dex+ MDA). The diffraction peaks are consistent with data file (JCPDS card No. 04- 0784) for all reflections.[5]

Stability study of GNP-formulations:

In order to understand the stability of GNP-formulationsF4 and F5, we prepared different type solutions say, 10% NaCl, 10% FBS, DPBS buffer, acidic pH solution, and basic pH solutions. Then F4 and F5 were kept into these solutions up to seven days at room temperature and measured UV-Vis spectra of these formulations at 1st and 7th day of incubation. Herein we observed in day one and day seven there was no significant change of UV-Vis λmax (either 5nm red or 5 nm blue shift or any significant absorbance) both F4 and F5, indicating GNP-formulations are sable in different solution up to seven day.

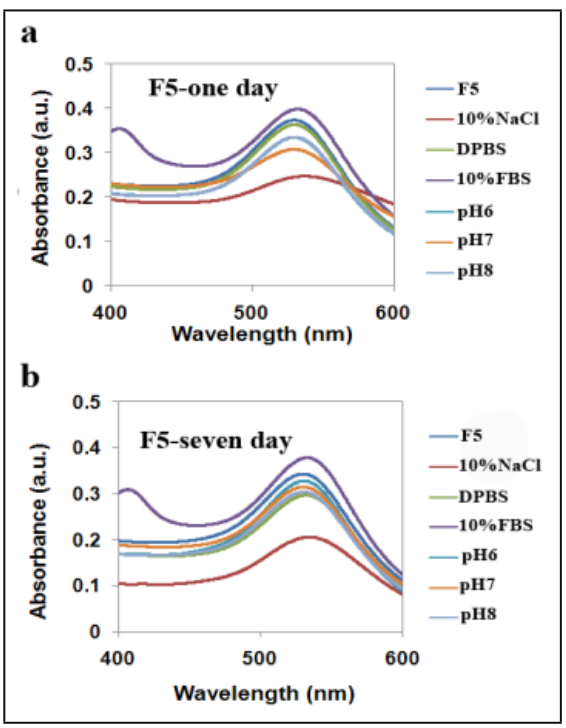

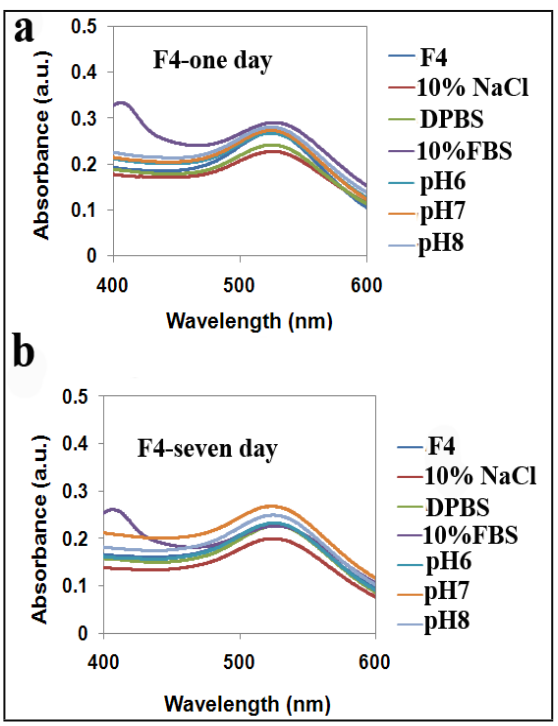

Figure S5: *In vitro* stability studies of F4 and F5 in different sets of solutions at first day and 7th days of incubation. Here we observed no significant change of λmax (either 5nm red or 5 nm blue shift) or absorbance (a.u.) at day one and day seven for both F4 and F5.

HPLC analyses of Dex in supernatant of centrifuged GNP

For Dex attachment to GNP, we formulated F3-F5 following a protocol as described earlier, followed by ultra-centrifugation (Sorvall™ WX Floor Ultracentrifuges, USA) with 18000rpm at 100C temperature. The supernatant of GNP-formulations were collected, lyophilized and solubilised in methanol for injection in HPLC (Varian prostarhplc, USA) at methanol running phase. For quantitative analysis, we made the calibration graph mimicking the condition of the actual experiment. Hence, for calibration, firstly we centrifuged the GNP and obtained the supernatant. The aliquots of supernatant were lyophilized and to it respective concentrations of Dex in methanol was added. Following which HPLC analyses of the standard Dex solutions and Dex in supernatant of F3-F5 were performed. However, the actual amount and % of Dex on GNPs were calculated by taking TGA data in account also (as described later).

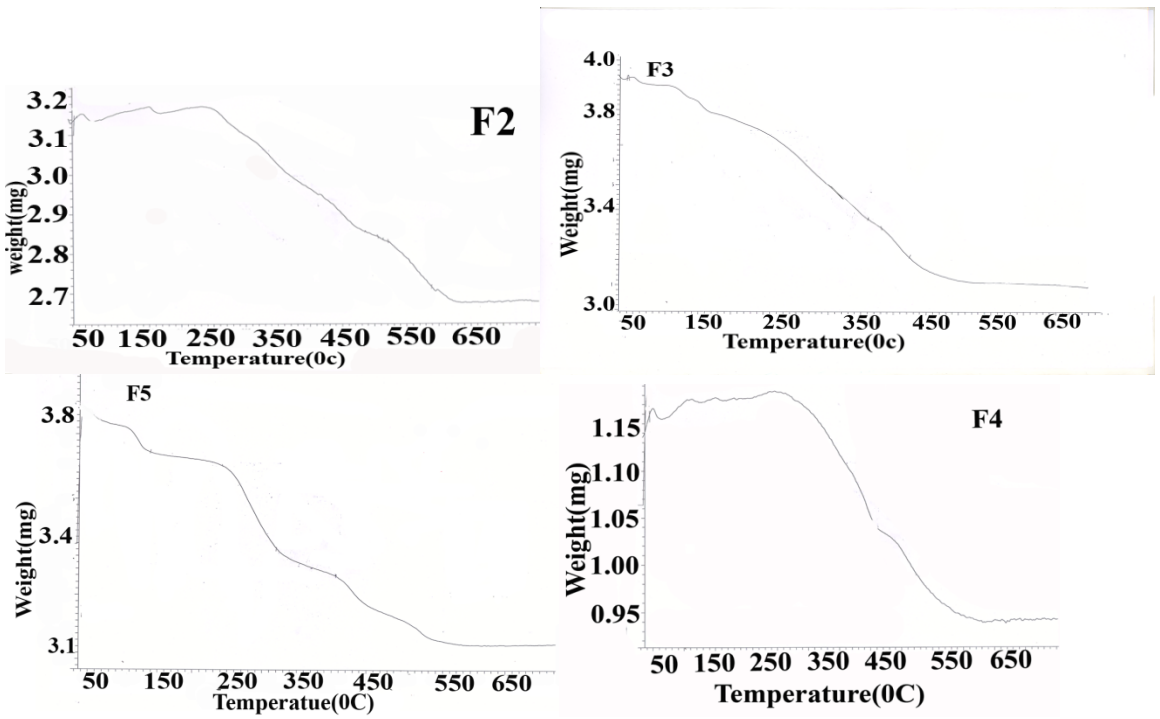

Figure S6: Thermo-gravimetric analyses of GNP formulations F3-F5.

Thermogravimetric Analysis (TGA) experiment

The weight loss (~15 % in F2, ~18 % in F3 & F4 and ~15 % in F5) around 250-500^{0}C in TGA data may be due to the covalent type bonding beteen Au and –SH in gold nanoformulation with MDA. [3, 4] Similarly, the weight loss around 100-150 ^{0}C in TGA data may be due to the presence of weaker interactions namely (i) noncovalent interaction (hydrophobic/ van der Waals/electrostatic) between –OH and GNP, and (ii) dative binding through non bonded electron transfer (n) may occur from carbonyl oxygen (=O) of Dex towards GNPs. Again, the weight loss around 200^{0}C – 500^{0}C reflects the strong polar covalent bonding may be due presence of Au-OH bond in F3-F5 formulations. According to Pauling's electronegativity theory, there is a chance for the formation of polar covalent bonding if difference of electronegativities between two atoms is less than 1.7 as more electronegative atom (partial negative charge) has a greater tendency to share of the bonding electrons than the less electronegative atom (partial positive charge). Here the difference of electronegativities between Au and O is 1.1 i.e. < 1.7 (enO = 3.5 and enAu = 2.4 i.e. the difference = 1.1) that suggest the formation of polar covalent bonding. The nature of bonding has been further confirmed by FTIR analysis.

Supplementary Table S1

Formulation	Total loading (%) in GNP formulations	Dex (%)	MDA (%)
F3	17.9	17.9	
F4	18.6	6.0	12.6
F5	15.0	8.6	6.4

Intracellular behavior of nanoparticles under long time exposure:

Dex and MDA-formulated GNP (F5) and MDA-formulated GNP (F2, where Dex is not present) were treated to A549 cells continuously for 10h respectively. GNP assembly inside the nucleus was very high in F5-treated cells but apparently no nuclear localization was observed in F2-treated cells even after 10h continuous treatment. F2 GNPs were by and large present in the cytoplasmic vesicle with higher density.

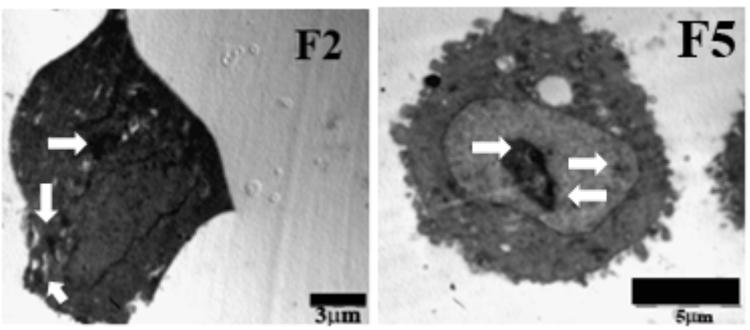

Figure S7: pattern of cellular internalization of F2 and F5-treated A549 cell for 10 h

RT-PCR study with pellet-out GNP formulations:

Herein, RT-PCR study was performed for observing GRE-gene (CYP3A5) regulation with respect to homing gene 18S. Firstly, GNP formulations F2-F5 were undergone ultra-centrifugation to obtain pellet out formulations respectively. A549 cells were then treated with F2-F5 pellets. They were also treated with F1 and free dex with equimolar concentration of Dex or kept untreated. The treated amount of F2 mimicked to that of F5. The total RNA isolated from respective groups were undergone RT PCR with CYP3A5 and 18S primer separately. The results are represented by gel electrophoresis of amplified DNA bands obtained from respective treated groups.

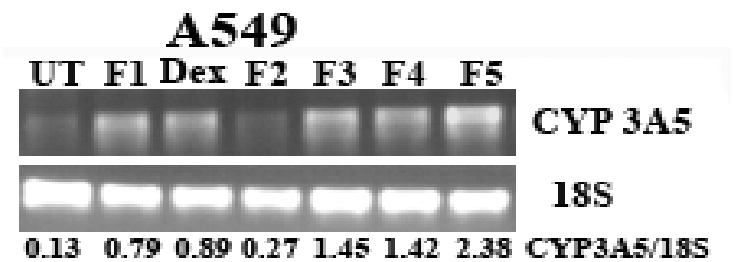

Figure S8: RT-PCR experiment in A549 cells treated with F1, free Dex and respective pellet-out GNP-formulations F2-F5.

Biodistribution of F5:

In preclinical study, we observed that the F5-treated mice had lesser tumor burden and significantly reduced tumor volume/weight than that of other treatment (F2-F4) or UT group [Figure 4A-C]. This observation is incidentally accompanied by increased acccumulation of GNP in tumors of F5-treated mice group compared to other organs. Tumors and other organs such as lungs, kidney, spleen were isolated from sacrificed mice after completion of in vivo tumor study. Thereafter GNPs in respective orgnas were quantified by ICP-MS analysis following the protocol as provided:

Bio-distribution of GNP using ICP-MS: Isolated organs and tumors were first weighed individually followed by digestion of these organs in 50% conc. HCl and HNO3. The respective mixtures were then heated over 90^0c water bath for 30', cooled down, added H_2O_2 and again heated, filtered and half-diluted with milliQ water before it is analysed by ICP-MS (model no. 7700X, made by Agilent Technology, USA).

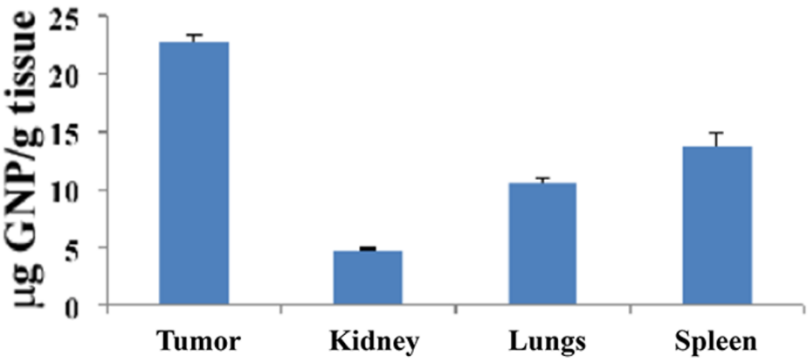

Figure S9: Bio-distribution of GNP of isolated tumor and organs, such as kidney, lungs, spleen treated with F5-formulation.

References

1. Weili, S.; Sahoo, Y.; Swihart, M.T. Gold nanoparticles surface-terminated with bifunctional ligands. Colloids and surfaces A: *Physicochem. Eng. Aspects*, 2004, **246**, 109-113

2. Hasan, M.; Bethell, D.; Brust, M. The Fate of Sulfur-Bound Hydrogen on Formation of Self-Assembled Thiol Monolayers on Gold: 1H NMR Spectroscopic Evidence from Solutions of Gold Clusters. *J. Am. Chem. Soc.* 2002, **124**, 1132-1133

3. Jang, N.H. The Coordination Chemistry of DNA Nucleosides on Gold Nanoparticles as a Probe by SERS. *Bull. Korean Chem. Soc.* 2002, **23**,1790-1800

4. S. Mukherjee, S.; Sushma, V.; Patra, S.; Barui, A.K.; Bhadra, M.P.; Sreedhar, B.; Patra, C.R. Green chemistry approach for the synthesis and stabilization of biocompatible gold nanoparticles and their potential applications in cancer therapy. *Nanotechnology*, 2012, 23, **455103**

5. Ghodake, G. S.; Deshpande, N. G.; Lee, Y. P.; Jin, E. S.; Pear fruit extract-assisted room-temperature biosynthesis of gold nanoplates. *Colloids surf. B Biointerfaces*, 2010, **75**, 584-589

6. Guo, Y.; Wang, Z.; Shao, H.; Jiang, X. Stable fluorescent gold nanoparticles for detection of Cu2+ with good sensitivity and selectivity. *Analyst*, 2012, **137**, 301-304

7. Weili, S.; Sahoo, Y.; Swihart, M.T. Gold nanoparticles surface-terminated with bifunctional ligands. colloids and surfaces A: *Physicochem. Eng. Aspects*, 2004, **246**, 109-113

8. Das, A.; Mukherjee, P.; Singla, S.K.; Guturu, P.; Frost, M.C.; Mukhopadhyay, D.; Shah, V.H.; Patra, C.R. Fabrication and characterization of an inorganic gold and silica nanoparticle mediated drug delivery system for nitric oxide. *Nanotechnology*. 2010, **21**, 305102

9. Patra, C.R.; Bhattacharya, R.; Wang, E.; Katarya, A.; Lau, J.S.; Dutta, S.; Muders, M.; Wang, S.; Buhrow, S.A.; Safgren, S.L.; Yaszemski, M.J.; Reid, J.M.; Ames, M.M.; Mukherjee, P.; Mukhopadhyay, D. Targeted delivery of gemcitabine to pancreatic adenocarcinoma using cetuximab as a targeting agent. *Cancer. Res*. 2008, **68**, 1970-1978